Procedures for Metabolomics and Lipidomics using Travelling Wave Ion Mobility Mass Spectrometry.

Giuseppe Paglia[1]; Giuseppe Astarita[2*]

1. European Academy of Bolzano/Bozen, Center for Biomedicine, Via Galvani 31, 39100 Bolzano, Italy
2. Department of Biochemistry and Molecular & Cellular Biology, Georgetown University, Washington, DC, USA.

Corresponding Authors: Giuseppe Paglia, giuseppe.paglia@eurac.edu and Giuseppe Astarita, gastarita@gmail.com

Abstract

Metabolomics and lipidomics aim to profile, in a comprehensive fashion, the wide range of metabolites and lipids that are present in biological samples. Recently, ion mobility spectrometry (IMS) has been used in support to metabolomics and lipidomics applications to facilitate the separation and the identification of complex mixtures of analytes. IMS is a gas-phase electrophoretic technique that enables the separation of ions in the gas phase according to their charge, shape, and size. Occurring within milliseconds, IMS separation is compatible with modern mass spectrometry (MS) operating with microsecond scan speeds. Thus the time required for acquiring IMS data does not affect the overall run time of traditional liquid chromatography (LC)/MS-based metabolomics and lipidomics experiments. The addition of IMS to traditional LC/MS-based metabolomics and lipidomics workflows has been showed to enhance peak capacity, spectral clarity, and fragmentation specificity. Moreover, by enabling determination of a collision cross-section (CCS) value—a parameter related to the shape of ions—IMS can improve the confidence of metabolite identification. In this protocol, we present standard operating procedures for integrating travelling wave ion mobility (TWIMS) into traditional LC-MS based metabolomic and lipidomic workflows using a SYNAPT mass spectrometer. In particular, we describe procedures for: tuning and calibration of the TWIMS-MS instrument; procedures for extraction of both polar metabolites and lipids from tissue samples; chromatographic conditions for the analysis of both polar metabolites and lipids; and metabolite identification using both TWIMS-derived fragmentation and CCS information using dedicated software such as Progenesis.

Keywords: lipidomics, metabolomic, collision cross section, drift time, travelling-wave IMS

INTRODUCTION

In recent years, ion mobility spectrometry (IMS) has been adopted increasingly as an additional tool for supporting traditional MS-based metabolomic and lipidomic workflows [1-14] (Figure 1). As a gas-phase electrophoretic technique, IMS enables the separation of ions within a chamber filled with a buffer gas and subjected to an electrical field[15-18]. The time required for ions to pass through the chamber relates directly to the shape, size, and charge of the ions as well as to the nature of the buffer gas. By allowing separations of ions on a timescale of milliseconds, IMS can be coupled with microsecond-scale mass spectrometry (MS) detection. Combining IMS and mass spectrometry (IMS-MS) significantly enhances analytical results. Compared with conventional, single-dimension MS analyses, IMS-MS generates cleaner mass-spectral data. In complex biological samples, it removes interferences[19, 20] and enhances peak capacity[20, 21], all of which increase confidence in metabolite identification or confirmation[5, 20-22].

Currently, four IMS-MS technologies are commercially available (Table 1):

1) drift-time IMS-MS (DTIMS- MS)[23];

2) travelling-wave IMS-MS (TWIMS-MS)[24, 25];

3) field asymmetric IMS-MS (FAIMS-MS) / differential mobility spectrometry (DMS)[26];

4) trapped IMS-MS (TIMS-MS)[27-29] .

The ion separation principles behind these IMS technologies have been previously reviewed in detail[15-18]. DTIMS and TWIMS instruments separate ions based on the time it takes for the ions to traverse the mobility cell, allowing all the ions to pass through the mobility cell. Since there is no need to select specific molecular targets, such devices are generally used for untargeted screening experiments. FAIMS/DMS devices separate ions by varying voltages, filtering ions in a space-dispersive fashion. TIMS-MS separates ions based upon differences in mobility, after trapping and selectively ejecting them[27-29].

Although IMS separation is often associated with loss in ion transmission and sensitivity, the overall effect on the limits of detection is hard to quantify in complex biological samples due to the fact that IMS also contribute to chemical noise reduction[18, 30, 31]..

IMS-MS has proven useful for analyzing large biomolecules, and protocols describing procedures for using it to characterize large protein complexes have been reported[32-34]. We recently reported the benefits achieved by integrating TWIMS in traditional MS-based metabolomic and lipidomic workflows[20-22, 35, 36] (Figure 1). The reproducibility of these procedures has been validated using instruments located in independent laboratories[20, 22]. Here, from the perspective of our laboratory's experience in the field, we provide experimental protocols for integrating TWIMS in MS-based metabolomics and lipidomics workflows using a SYNAPT mass spectrometer instrument.

TWIMS-derived information

The combination of TWIMS with traditional analytical approaches offers these major advantages for metabolomics and lipidomics:

- Additional post-ionization separation capability – Provides increased peak capacity, cleaner mass-spectral data, and increased signal-to-noise ratio for complex mixtures of metabolites in biological samples.
- Collision cross section (CCS)-measurement capability – The CCS, based on the shape of metabolites, provides for each analyte a third physicochemical parameter (in addition to mass and retention time) that increases the confidence of metabolite identification.
- Specificity of metabolite identification – Coupling MS/MS fragmentation with TWIMS, adds a new set of tools for structural characterization, improving the specificity of metabolite identification.

Additional post-ionization separation capability Identifying lipids and metabolites remains one of the most challenging steps involved in analyzing biological samples[37-43]. IMS can help in the identification

process. In a direct infusion experiment, the additional dimension of separation in an IM-MS experiment increases the peak capacity sixfold over a more traditional MS-only experiment[20]. Theoretically, in TWIM-MS instruments such as SYNAPT, the activation of TWIMS capabilities should not affect sensitivity, since all ions should pass through the ion mobility separation cell before TOF detection. However, because of ion diffusion and conductance in the high-to-low pressure interfaces, a modest decrease in the sensitivity of detection can be observed, which is hard to quantify since the signal-to-noise increase at the same time. Data generated from an IM-MS experiment can be plotted, the *x* axis representing mobility, the *y* axis mass. Doing so differentiates metabolites and lipids from other classes of biomolecules, such as peptides, carbohydrates, and oligosaccharides, and from chemical noise [44-46]. Different chemical classes fall into distinct areas and trend lines on an *m/z*-mobility plot, facilitating the feature annotation and identification of lipids and metabolites [4, 11, 20, 22, 45, 47-49] (Figure 2a,b).

The capability of IMS to increase peak capacity is even more evident during MS imaging (MSI) experiments[20]. Coupling IMS with MSI workflows separates lipid and metabolite ions from interfering background peaks. In fact, lipids and metabolites fall into distinct areas which might also help to separate chemical noise[20]. Separation is achieved according to the ions' charge, size, and shape, before they undergo mass detection. For example, DESI IMS-MSI was recently used to image, directly from murine, brain tissue, multiply charged ganglioside species, thus separating them, according to charge state, from the remaining lipid classes[50]. In addition to MSI, other experiments involving direct analysis using ambient ionization techniques coupled with IMS-MS are equally instructive. For high-throughput fingerprinting of biological samples, they have been shown to improve the rapid screening and detection of lipids and metabolites directly from solid or liquid samples[36, 37].

IMS-derived CCS

In addition to measuring *m/z*, IMS devices, such as DTIMS and TWIMS, can provide the rotationally averaged CCS of an ion [15, 17, 51]. CCS values can be calculated from the time required for an ion to cross the mobility separation cell. The CCS represents the effective area for the interaction between an individual ion and the neutral gas through which it travels. An important physicochemical property, the CCS can be useful in identifying an ion in the gas phase according to its chemical structure and three-dimensional conformation. The CCS of a compound is independent of the nature and complexity of the analytical sample and it can be measured, regardless of the sample matrix and experimental conditions with high reproducibility. Thus, the use of CCS values, in addition to other molecular identifiers such as retention time (RT) and mass-to-charge ratio (*m/z*), provides an orthogonal coordinate that increases the specificity of metabolite identification.

In DTIMS-MS devices with a uniform electrostatic field, CCS can be directly derived from the drift time[52, 53]. In TWIMS-MS instruments, to which an electric-field waveform function is applied, procedures to experimentally calculate the CCS are based on IMS calibration performed using compounds of known CCS under defined conditions (i.e., gas type and pressure, travelling wave speed or height) [44, 54-56].

We previously showed that CCS calibration corrects for the variation in drift times among TWIMS-MS instruments in independent laboratories, where the instruments' ion-mobility parameter settings vary, resulting in highly reproducible measurements[20, 22, 55]. We also demonstrated that CCS values for more than 250 lipids and 125 metabolites are unaffected by instrument settings or chromatographic conditions, and they are highly reproducible on instruments located in geographically separated independent laboratories[20, 22]. Metabolites and lipids can be searched against a three-coordinate database that includes retention time, molecular mass, and CCS values, to increase the confidence of identification and reduce the number of false positive and negative identifications[20, 22]. CCS values have been also proven to be

highly reproducible in various matrices[20]. Nevertheless, we cannot exclude at the moment that very low concentration of some specific metabolites or very noisy matrices might affect CCS measurements.

During direct-analysis experiments relying exclusively on mass values, when no chromatographic separation is present, the presence of isobaric and isomeric species can confound the interpretation of spectra and increase the number of false positive identifications. Databases that include CCS values for lipids and metabolites have proven valuable for MS imaging studies. Combining mass measurements with CCS data reduces the number of candidates that may map to each *m/z*, increasing the confidence in the identification. Furthermore, the combined extraction of both *m/z* and CCS values has been shown to increase the signal-to-noise ratio and improve the spatial localization of lipids in tissues[20].

Fragmentation coupled with TWIMS separation using a SYNAPT system

In metabolomics and lipidomics, the identification of chemical structures often relies on fragmentation spectra obtained using different MS/MS modes of acquisition, including multiple reaction monitoring (MRM), data-dependant acquisition (DDA) and data-independent acquisition (MS^E) modes of acquisition. In biological samples, however, thousands of metabolites and lipids exist, many of which can co-elute at the same retention time or appear in similar regions of the *m/z* scale. Applying MS^E to these samples would yield MS/MS spectra containing a mixture of collision-induced fragment ions derived from multiple co-eluting precursors, complicating the interpretation of the spectra. To help identify complex mixtures of metabolites, taking advantage of the geometrical configuration of the SYNAPT system, precursor ions can be fragmented after the TWIMS separation. Combining TWIMS with MS^E provides for separating co-eluting precursor ions before fragmentation, according to their drift times. The result is cleaner MS/MS product-ion spectra, increased specificity, and reduced false-positive assignments [1, 2, 5, 19-22, 57].

For complex chemical structures, multiple fragmentation cycles are often used. The particular geometrical

configuration of instruments in a SYNAPT system, where collision cells are placed one before and one after the TWIMS cell, effects a pseudo-MS^3 mode of acquisition commonly referred to as "time-aligned parallel," or "TAP," fragmentation [5]. Such a mode of acquisition allows selection of a precursor ion of interest by means of the quadrupole mass filter and then subjecting it to pre-TWIMS fragmentation in the first collision cell. A packet of fragment ions so produced can then be subjected to TWIMS separation followed by secondary post-TWIMS fragmentation in the second collision cell. Association of secondary fragment ions to specific drift times of primary fragment ions allows producing pseudo-MS^3 spectra. TAP fragmentation has been used to characterize the structure of complex lipids in a single analytical step[5].

Integration of TWIMS in a traditional LC-MS protocol

Chromatographic separations are routinely coupled with MS to resolve complex mixtures of analytes. Biological samples, however, contain several thousands of metabolites, representing a challenge even for chromatographic systems to completely resolve. Because chromatographic separations occur in seconds and TWIMS separations in milliseconds, TWIMS can be coupled with chromatography. Such a coupling provides an additional degree of separation. It increases peak capacity, distinguishes metabolites from matrix interferences, helps generate cleaner mass spectral data, and even confers the ability to resolve structural isomers [2, 56, 58]. The data sets generated from a typical UPLC-TWIMS-MS experiment include CCS values as well as retention-time and mass (that is, *m/z*) values. CCS values are more reproducible than RT values. The latter might shift, owing to the nature of the analytical matrix; the chromatographic conditions, such as column degradation; batch-to-batch compatibility of mobile phases; and sample loading. Thus CCS values provide a third, orthogonal coordinate for metabolite identification in addition to retention time and accurate mass. This additional assurance can improve confidence in metabolomics studies by reducing the number of potential false-negative and false-positive identifications (Figure 2) [1, 10, 14, 20, 22].

MATERIALS

REAGENTS

- Natural lipids and lipid extracts (Avanti Polar Lipids) (Table 2).
- Poly-DL-alanine (Sigma-Aldrich, USA; catalogue number p9003).
- CCS Major Mix calibration solution (Waters, catalogue number 186008113).
- LCMS QCRM mix (Waters, catalogue number 186006963), which is a component mix of acetaminophen, caffeine, sulfaguanidine, sulfadimethoxine, valine,-tyrosine-valine, verapamil, terfenadine, leucine-enkephalin and reserpine.
- TWIMS System Suitability LipidoMix® Kit (Avanti Polar Lipids, catalogue number 791500).
- Leukine enkephalin (Sigma-Aldrich, catalogue number L9133).
- Sodium formate (Sigma-Aldrich, catalogue number 17841).
- Acetic acid (Sigma-Aldrich, catalogue number 49199). CAUTION Acetic acid is corrosive and highly flammable and should be handled in a fume hood.
- Ammonium formate (Sigma-Aldrich, catalogue number 14266) CAUTION Ammonium formate causes skin irritation and serious eye irritation.
- Formic acid (Sigma-Aldrich catalogue number 56302) CAUTION Formic acid is corrosive and volatile and should be handled in a fume hood.
- Isopropanol (Sigma-Aldrich, catalogue number 34965) CAUTION Isopropanol is harmful and highly flammable and should be handled in a fume hood.
- Methanol (Sigma-Aldrich, catalogue number 34860) CAUTION Methanol is harmful and highly flammable and should be handled in a fume hood.
- Acetonitrile (Sigma-Aldrich, catalogue number 34851) CAUTION Acetonitrile is harmful and highly flammable and should be handled in a fume hood.
- Chloroform (Sigma-Aldrich, catalogue number 650498) CAUTION Chloroform is harmful and toxic and should be handled in a fume hood.

- Frozen human brain samples (frontal cortex) were obtained from the Banner Sun HealthResearch Institute (Sun City, AZ). CAUTION Adhere to all relevant ethical regulations and guidelines for the collection and use of human blood. CAUTION To avoid potential contact with pathogens, perform all work with appropriate personal protection equipment including gloves and glasses.
- Arachidonic acid d8 (Sigma-Aldrich, catalogue number 735000).
- Cholesterol-d7 (Sigma-Aldrich, catalogue number 677574).
- C17:0-cholesteryl ester (Avanti Polar Lipids, catalogue number 110864).
- 1,2-dimyristoyl-*sn*-glycero-3-phosphoethanolamine (Avanti Polar Lipids, catalogue number 110632).
- 1,2-dimyristoyl-*sn*-glycero-3-phosphocholine (Avanti Polar Lipids, catalogue number 850345).
- 1-heptadecanoyl-2-hydroxy-*sn*-glycero-3-phosphocholine (Avanti Polar Lipids, catalogue number 855676).
- Phenylalanine d2 (Sigma-Aldrich, catalogue number 615889).
- Succinate d4 (Sigma-Aldrich, catalogue number 341371).
- Glucose $^{13}C_6$ (Sigma-Aldrich, catalogue number 389374).
- Carnitine d9 (Sigma-Aldrich, catalogue number 729868).
- Glutamic acid d5 (Sigma-Aldrich, catalogue number 616281).
- Lysine d4 (Sigma-Aldrich, catalogue number 616192).
- Alanine d4 (Sigma-Aldrich, catalogue number 485845).
- Nicotinamide (Sigma-Aldrich, catalogue number 72340).
- 5-oxoproline (Sigma-Aldrich, catalogue number 83160).
- Phenylalanine (Sigma-Aldrich, catalogue number 78019).
- Succinic acid (Sigma-Aldrich, catalogue number S3674).
- Hypoxanthine (Sigma-Aldrich, catalogue number H9377).
- Arginine (Sigma-Aldrich, catalogue number W381918).

- Inosine (Sigma-Aldrich, catalogue number I4125).
- SAH (Sigma-Aldrich, catalogue number A9384).
- Raffinose (Sigma-Aldrich, catalogue number R0514).

EQUIPMENT

- Liquid chromatography system, such as an ACQUITY UPLC® I-Class System (Waters Corporation).
- MS system: SYNAPT High Definition Mass Spectrometry (HDMS) (Waters Corporation).
- UPLC column: ACQUITY UPLC Charged Surface Hybrid (CSH™) C18 (2.1 × 100 mm) 1.7 µm (Waters Corporation).
- UPLC column: ACQUITY UPLC BEH Amide Column (2.1 × 150 mm) 1.7 µm (Waters Corporation).
- Glass tubes with caps, including a PTFE-covered liner.
- Ar (>99.9%, vol:vol).
- He (>99.9%, vol:vol).
- N_2 (99.9%, vol:vol). CRITICAL STEP. Routinely, TWIMS measurements are made using nitrogen (N_2). Nevertheless, TWIMS resolution can be optimized using other gases. The SYNAPT G2-Si and SYNAPT G2-S instruments can be used with 12 different TWIMS gases: (nitrogen (N_2), argon (Ar), carbon dioxide (CO_2), carbon monoxide (CO), helium (He), hydrogen (H_2), neon (Ne), nitrogen dioxide (NO_2), nitrogen oxide (N_2O), oxygen (O_2), sulfur hexafluoride (SF_6). In all cases, the gas purity must be at least 99.5%. Note that some gases warrant consideration of special safety measures, regulators, and handling practices.
- MassLynx® software (Waters) is used to acquire data for the SYNAPT HDMS system.
- Progenesis® QI (Nonlinear Dynamics, Newcastle, UK) is used for processing and analyzing TWIMS information for both qualitative and quantitative applications.

- DriftScope™ software (Waters) is used to extract regions of interest for different molecules on the basis of selective drift-time extraction of mass spectra.

PROCEDURE

TWIMS-MS parameters: setting and optimization and calibration

1 To optimize TWIMS-MS settings for polar metabolites, choose option A, below. To optimize TWIMS-MS settings for lipids, choose option B.

Option A: optimizing TWIMS-MS settings for polar metabolites **TIMING 1 – 3 h**

(i) Prepare a system-suitability standard solution for polar metabolites at 10 µg/mL in water/acetonitrile 50:50 (vol:vol). We suggest a mixture containing nicotinamide, 5-oxoproline, phenylalanine, succinic acid, hypoxanthine, arginine, inosine, SAH, and raffinose

CRITICAL STEP Select the metabolite of your system-suitability standards solution considering the mass range you want to use during the analysis of real samples.

(ii) Directly infuse the system-suitability standard solution for polar metabolites at 5 µL/min, in both the ES+ and ES- ionization mode, adjusting TWIMS-MS parameter settings to control TWIMS-MS separation[59].

(iii) Optimize TWIMS-MS settings. Set the mass spectrometer on Mobility-TOF and start from the settings given in Table 4. These setting were optimized using a mixture of small polar metabolites. The two main parameters that could require tuning to achieve optimal TWIMS separation using a SYNAPT HDMS system are:

a) Wave velocity in the TWIMS cell – Increasing the T-wave velocity will widen the drift time distribution profile

b) Wave height in the TWIMS cell – Increasing the T-wave height will narrow the distribution profile.

Ensure that all masses of interest fit in the TWIMS separation window by increasing and decreasing the T-wave velocity and T-wave height.

(iv) Visualize data in DriftScope software via the 2D plot (*m/z* vs drift time). Ensure that all

masses of your system-suitability standard solution were detected. If separation of isomers and/or isobars is required and is not achieved after TWIMS settings optimization refer to Troubleshooting. If the same ion peaks are detected at the beginning and at the end of the driftogram refer to Troubleshooting. If diagonal strips appear in the 2D plots (drift time vs retention time) refer to Troubleshooting.**TROUBLESHOOTING**

Option B: optimizing TWIMS-MS settings for lipids **TIMING 1 – 3 h**

(i) For reference samples, we suggest using brain (porcine) lipid extract as system-suitability standards, to confirm visualization and separation of the wide range of lipid classes present in biological samples (other commercially available lipid extracts are reported in Table 2)

CAUTION Use glass tubes with caps that include a PFTE-covered liner, to avoid leaching contaminants into organic solutions.

CRITICAL STEP If you decide to prepare a different solution for a system-suitability standard, select the lipids of interest considering the mass range you will use during the analysis of real samples.

(ii) Directly infuse the brain (porcine) lipid extract at 5 µL/min, in both the ES+ and ES- ionization modes, adjusting TWIMS parameter settings to control TWIMS separation[59].

(iii) Optimize TWIMS settings. Set the mass spectrometer on Mobility-TOF and start from the settings given in Table 5. These setting were optimized using brain porcine extract from Avanti Polar. The two main parameters that could require tuning to achieve optimal TWIMS separation using a SYNAPT HDMS system are:

(a) Wave velocity in the TWIMS cell – Increasing the T-wave velocity will widen the drift time distribution profile

(b) Wave height in the TWIMS cell – Increasing the T-wave height will narrow the distribution profile.

Ensure that all masses of interest fit in the TWIMS separation window by increasing and decreasing the T-wave velocity and T-wave height.

(iv) Visualize data in DriftScope software via the 2D plot (*m/z* vs drift time). Ensure that all masses of your system-suitability standard solution were detected. If separation of isomers and/or isobars is required and is not achieved after TWIMS settings optimization refer to Troubleshooting. If separation of isomers is not achieved refer to Troubleshooting. If the same ion peaks (same *m/z*) are detected at the beginning and at the end of the driftogram refer to Troubleshooting. If diagonal strips appear in the 2D plots (drift time vs retention time) refer to Troubleshooting. **TROUBLESHOOTING**

Preparing poly-DL-alanine solution **TIMING** 10 min

2 Prepare a fresh solution of poly-DL-alanine at 10 µg/mL. **TROUBLESHOOTING**

3 Perform instrument calibration and performance checks, or both, according to the instrument manufacturer's guidelines. **TIMING** 2 h

CRITICAL STEP Allow the mass spectrometer to remain in Operate mode for at least 1 hour prior to CCS calibration to ensure a stable calibration.

4 To perform a manual procedure for CCS calibration, choose option A, below. To perform an automated procedure, choose option B.

Option A: deriving CCS using a manual procedure **TIMING 1 h**

(i) Inject the solution of poly-DL-alanine (alternatively, you can use the CCS Major Mix solution) at 10 µL/min using the experimental conditions previously set. In the software, confirm that the beam is stable. Confirm that you can clearly observe the ion at 232.1 *m/z* by enlarging the low-*m/z* range of the spectrum window.

CRITICAL STEP TWIMS parameter settings used during poly-DL-alanine calibration and those used to obtain CCS for standard compounds and unknown lipids

and metabolites must be identical.

(ii) Annotate the drift time of the standards determined at the apex of the TWIMS peak in both ES^+ and ES^- ionization modes.

(iii) Subtract instrumental offsets. This correction factor (c) can be found in the MassLynx Tune windows, subtract instrumental offsets. Click System > Acquisition Settings. Then, on the Acquisition Setup tab, click EDC delay (mass <5000 Da). The value for the correction factor = c (the enhanced duty-cycle delay coefficient), usually falls between 1.4 – 1.6.

(iv) Calculate the corrected drift time: $t_d' = t_d - (c\sqrt{}\ (m/z <ion> / 1000)$ ms.

(v) To obtain calibration coefficients, use cross-section data (Ω) for singly charged poly-DL-alanine oligomers (Table 3).

CRITICAL STEP These CCS values were obtained using nitrogen. If you plan to use helium, you will need CCS for singly charged poly-DL-alanine oligomers obtained by using helium[55].

(vi) Correct published cross sections by accounting for reduced mass and charge state. Reduced mass: $\mu = (M_{ion} \times m_{gas} / M_{ion} + m_{gas})$

(vii) Calculate the normalized cross-section: $\Omega' = [\Omega \times \sqrt{(\mu)}]/z$

(viii) Plot t_d' versus Ω', and fit a power-trend line of the form $y = Ax^b$ to the data, to obtain a calibration curve.

Option B: deriving CCS using an automated procedure **TIMING 30 min**

(i) Using the instrument's IntelliStart feature, select CCS calibration. Infuse the poly-DL-alanine or CCS Major Mix solution into the analyte probe, and confirm that the beam is stable. Ensure that you clearly see the complete range of *m/z* that you expect to use for the calibration. In the case of poly-DL-alanine, inspect the peaks of the singly charged oligomers reported in Table 3. Acquire calibration data automatically via IntelliStart,

and accept the calibration if the %RMS CCS is below 1%.

(ii) Use the instrument's LockCCS function to set up. Immediately after the CCS calibration, perform the LockCCS by infusing leukine enkephalin at 10 µL/min. Use IntelliStart, and select LockSpray source setup. Start flow, and verify that $[M+H]^+$ or $[M-H]^-$ ions of leukine enkephalin can be seen in the Tune window. IntelliStart then acquires data automatically.

5 Directly infuse the porcine-brain lipid extract at 5 µL/min, in both the ES+ and ES- ionization modes, and convert experimental effective drift times to estimated collision cross-sections using the calibration curve. **TROUBLESHOOTING TIMING 30 min**

6 Directly infuse the system-suitability standard solution for polar metabolites at 5 µL/min (in both ES+ and ES- ionization modes), and convert experimental, effective drift times to estimated collision cross sections using the calibration curve. **TROUBLESHOOTING TIMING 30 min**

LC/MS analysis setup

7 To optimize the LC settings for analyzing polar metabolites, choose option A, below. To optimize the LC settings for analyzing lipids, choose option B.

Option A: optimizing LC settings for analyzing polar metabolites **TIMING 2 h**

(i) Prepare mobile phases A and B.

(a) Mobile phase A: acetonitrile with 0.1% formic acid

(b) Mobile phase B: water with 0.1% formic acid

(ii) Insert the column in the column compartment. We suggest to use the (2.1 × 150 mm) ACQUITY UPLC BEH Amide column, particle size 1.7 µm.

(iii) Set the column temperature at 45°C, the flow rate at 0.4 mL/min, the injection volume at 5 µL, and the autosampler temperature at 4°C.Set gradient conditions. . Use the following elution gradient: 0 min, 99% A; 6 min, 40% A; 8 min, 99% A; 10 min, 99% A.

(i) Use as weak wash solvent, acetonitrile:water (90:10, vol:vol), and, as strong wash solvent acetonitrile:water (40:60, vol:vol).

(ii) Equilibrate the column, running the gradient four times without injecting sample.

Option B: optimizing LC settings for lipidomics **TIMING 2 h**

i. Prepare mobile phases A and B.

(a) Prepare mobile phase A: acetonitrile:water (60:40, vol:vol) with 10mM ammonium formate and 0.1% formic acid.

(b) Prepare mobile phase B: isopropanol:acetonitrile (90:10, vol:vol) with 10mM ammonium formate and 0.1% formic acid.

ii. Insert the column in the column compartment. We suggest using the ACQUITY UPLC CSH C_{18} column, 100 × 2.1 mm (inner diameter), particle size 1.7 µm.

iii. Set the column temperature at 55°C, the flow rate at 0.4 mL/min, the injection volume at 5 µL, and the autosampler temperature at 10°C.

CRITICAL STEP Setting the autosampler to a temperature lower than 10°C could cause lipid precipitation.

(iv) Set gradient conditions. Use the following elution gradient: 0 min, 60% A; 2 min, 57% A; 2.1 min, 50% A; 12 min, 46% A; 12.1 min, 30% A, 18 min, 1% A; 18.1 min 60% A, 20 min, 60% A.

(v) Use as weak wash, acetonitrile:water:isopropanol (30:30:40, vol:vol:vol), and, as strong wash, a mixture of isopropanol:water:formic acid:dichloromethane (92:5:2:1, vol:vol:vol:vol)

(vi) Equilibrate the column, running the gradient four times without injecting sample.

Data-independent acquisition coupled with TWIMS TIMING 30 min

8 The $HDMS^E$ mode provides two distinct functions (Figure 5b) that must be set separately:

Function 1 (Low Energy)

Function 1 provides precursor ion information (Figure 5b). During function 1, ions are not dissociated by means of low collision-energy values, yet they are separated by IMS (Figure 5b).

(i) Set collision energy in the trap cell to 5 eV.

(ii) Set the parameter in the TWIMS cell, as reported in Table 4 or Table 5, or as previously optimized, in step 1A or 1B.

(iii) Set the collision energy in the transfer cell at 5 eV.

Function 2 (High Energy)

Function 2 (High Energy) provides product-ion information. Ions are first separated in the TWIMS cells and then dissociated by collisional events occurring in the transfer cells.

(i) Specify the collision energy for the trap cell as 5 eV.

(ii) Specify the parameter setting for the TWIMS cell as reported in Table 4 or Table 5, or as previously optimized, in step 1A or 1B.

(iii) Ramp collision energy in the transfer cell (we suggest to between 20 and 40 eV.)

CRITICAL STEP For optimal peak picking, data must be acquired in continuum mode.

Sample analysis

9 Prepare an ice-cold methanol solution containing a mixture of the internal standards. For example: d8 arachidonic acid (0.1 µg/mL), cholesterol-d7 (50 µg/mL), C17:0-cholesteryl ester (1 µg/mL), 1,2-dimyristoyl-sn-glycero-3-phosphoethanolamine (10 µg/mL), 1,2-dimyristoyl-sn-glycero-3-phosphocholine (10 µg/mL), 1-heptadecanoyl-2-hydroxy-sn-glycero-3-phosphocholine (1 µg/mL), phenylalanine d2 (1.5 µg/mL), succinate d4 (1.5 µg/mL), glucose 13C6 (60 µg/mL), carnitine d9 (0.15 µg/mL), glutamic acid d5 (1.2 µg/mL), lysine d4 (1.5 µg/mL), alanine d4 (3 µg/mL). TIMING 1 h

10 Weigh frozen tissue samples (20 mg), and homogenize them in 1 mL of ice-cold methanol containing internal standards. **TIMING** **30 min**

11 Extract lipids and metabolites by adding 1 mL of chloroform: water (2:1, vol:vol). Vortex-mix for 2 min, and centrifuge at 10,000x*g* for 10 min, 4˚C. **TIMING** **20 min**

12 Recover the upper phase (polar metabolites) and the bottom phases (lipids), and dry both phases in a centrifugal vacuum evaporator to dryness. **TIMING** **2-3 h**

13 To analyze polar metabolites, choose option A. To analyze lipids, choose option B.

Option A: Analysis of polar metabolites.

(i) Reconstitute dried polar metabolites samples (upper phase) in 200 µL of acetonitrile:water (1:1, vol:vol).

(ii) Prepare "pooled QC" samples by pooling a small aliquot (10 µL) from each extracted samples.

(iii) Use the system-suitability standards solution described in step 1A (i) as CCS QC standard solution Ensure precise CCS measurements by running the QC prior to sample analysis.

(iv) Prepare a sample list. Include samples in randomized order, a "pooled QC sample," and a CCS QC standard solution.

(v) Inject pooled QC samples 10 times, to stabilize the UPLC-TWIMS-MS system.

(vi) Run the samples.

(vii) Use the pooled QC samples and CCS QC standard solution to verify the reproducibility of the analysis, thus evaluating retention time, intensity, mass accuracy, and confirming that CCS (N_2) measurements fall within 2% of expected values.

Option B: Analysis of lipids.

(viii) Reconstitute dried lipids samples in 100 µL of isopropanol/acetonitrile/water 4:3:1 (vol:vol:vol).

(ix) Prepare CCS QC standard solution by diluting LCMS QCRM mix, 1:100, using isopropanol:acetonitrile:water 4:3:1 vol:vol:vol). Ensure precise CCS measurements by running the QC immediately prior to sample analysis. Alternatively, the LipidoMix from Avanti can be used to determine the TWIMS system suitability.

(x) Prepare "pooled QC" samples by pooling a small aliquot (10 µL) from each extracted samples.

(xi) Prepare a sample list. Include samples in randomized order, a "pooled QC sample" and a CCS QC standard solution.

(xii) Inject pooled QC samples 10 times, to stabilize the UPLC-TWIMS-MS system.

(xiii) Run the samples.

(xiv) Use the pooled QC samples and CCS QC standard solution to verify the reproducibility of the analysis, evaluating retention time, intensity, mass accuracy, and confirming that CCS (N_2) measurements fall within 2% of expected values.

Data processing and analysis TIMING 1-6 h

14 Import the UHPLC-TWIMS-MS data into Progenesis® QI software. Data are converted in an ion-intensity map, in which each MS signal is mapped by *m/z* and retention time.

15 Align ion maps in the retention-time direction, and perform peak picking. From the aligned runs, Progenesis QI software produces an aggregate run that represents the compounds in all samples, and it uses the aggregate run for peak picking. The peak picking from this aggregate is then propagated to all runs, so that the same ions are detected in every run. Data are normalized according to commonly used methods including total-ion intensity.

16 Progenesis QI software is coded to automatically convert drift-time data into CCS values using the calibration curve that appears in each raw-data folder. Features are automatically deconvoluted for isotopes and adducts; each feature is associated with a specific RT, *m/z* and CCS value.

17 Perform univariate, multivariate, or both types of statistical analyses.

18 Select features of interest according to significance (e.g . use a p-value of 0.05 to select discriminating features).

19 Search the selected features in databases containing CCS information by matching experimentally-derived CCS values against CCS databases[20, 22]. Databases containing CCS for several polar metabolites and lipid species are available in the literature [20, 22].

TROUBLESHOOTING

The difference between reference CCS (contained in the database) and experimental CCS values (ΔCCS) contributes to the identification score, in addition to accurate masses, isotopic pattern and retention times. Fragmentation spectra can be analyzed in $HDMS^E$ mode.

20 Lipids and polar metabolites can be searched by selecting a ΔCCS that is less than that of a given threshold as tolerance parameters (we suggest to use a ΔCCS<2%)[20, 22].

21 Filter and score identifications when querying the database with CCS information to reduce the number of false positives and negatives[22].

22 Confirm metabolite and lipids identification by matching fragmentation profiles obtained in HDMSE (Function 2 at high energy) with MSMS spectra available in-house or in public databases including HMDB[60], LipidBlast[61], and METLIN®[62].

Time-aligned parallel (TAP) fragmentation TIMING 1 h

23 Perform instrument calibration and performance checks, or both, according to the instrument manufacturer's guidelines.

24 Using the quadrupole mass filter, select a specific precursor-ion metabolite or lipid of interest

25 Fragment the selected analytes in the first collision cell (the trap cell) before the mobility separation.

26 Ramp collision energy in the trap cell (we suggest to between 20 and 40 eV).

27 Separate the fragmented ions by TWIMS. For the TWIMS cell parameter setting, specify the value reported in Table 4 or Table 5.

28 Further perform an additional fragmentation step in the second collision cell (transfer cell), located after the TWIMS separation cell. Ramp collision energy in the transfer cell (we suggest to between 20 and 40 eV).

29 Open data in DriftScope software.

30 From the File menu, select “Export drift time in MassLynx.” Open the exported driftogram in MassLynx. Fragment ions generated in the Trap Cell are then separated by ion mobility and will show different drif time. Open the peak of each fragment and visualize the pseudo-MS^3 data generated. **TROUBLESHOOTING**

ANTICIPATED RESULTS

Figure 4 and Figure 5 present the high level of information derived from a typical UPLC-TWIMS-HDMSE analysis of lipids extracted from brain tissue. Such an untargeted lipidomics analysis provided thousands of lipid features (Figure 4a). Each feature is characterized by three coordinates, *m/z,* retention time, and drift time. By using dedicated software, such as Progenesis QI, it is possible to automatically convert the drift time in CCS (Figure 4b). Both *m/z* and CCS are unique physicochemical features associated with each specific lipid molecule. On the other hand, retention-time measurements are strictly related to the LC settings, and moreover it is subject to shifting, because of the nature of the analytical matrix, the degradation of the chromatographic column, batch-to-batch compatibility of the mobile phases, and sample loading. Adopting CCS in addition to retention time and *m/z* allows use of a three-coordinate matching database search. Consequently, it allows us to widen the tolerance windows of database matching, ultimately decreasing the numbers of false-positive and false-negative identifications[20, 22, 36] (Figure 4b).

Lipid identifications can then be further confirmed by means of the cleaner fragmentation spectra obtained by exploiting the HDMSE capability of such a workflow (Figure 5). HDMSE, function 1 (low-collision cell energy), provides information about the precursor ions. Function 2 (high-collision cell energy) provides fragment-ions information, separated into three dimensions, for each feature. For example, identifying L-phosphatidylethanolamine (PE) as the 18:0/22:6 would have been difficult in a classical data-independent acquisition workflow because multiple PE species co-elute at the same retention time, producing a mixture of fatty acyl chains as fragments (Figure 5). In particular, three species are fragmented simultaneously resulting in four fragments representing the cleavage of 4 different the fatty acyl moieties (Figure 5a). The integration of TWIMS in this workflow provides an additional separation step, enabling the separation of coeluting PE species before fragmentation. Once separated by TWIMS, these species are selectively fragmented, providing specific fragment useful for lipid confirmation. Indeed, working in HDMSE mode, we show that the ion at *m/z* 790.5381 generated two

548 fragments, at *m/z* 327.2309 and 283.2616, which are, respectively, the FA (22:6) and the FA (18:0),
549 allowing us to confirm the PE (18:0/22:6).
550
551 **AUTHOR CONTRIBUTION STATEMENTS**
552 GP and GA designed the protocol, performed the experiments and wrote the manuscript.
553
554 **ACKNOWLEDGEMENTS**
555 This work was partially supported by the Alzheimer's Association (NIRG-11-203674 to G.A.).
556 We would like to thank Drs. David Grant, Andrea Armirotti, Will Thompson, Michal Kliman,
557 Hans Vissers, Kevin Giles, Jonathan Williams, Nick Tomczyk, Sigurdur Smarason, Alessia
558 Foglio, Michele Tarquinio, Bindesh Shrestha and Suraj Dhungana for discussions we found most
559 enlightening. We are grateful to the Banner Sun Health Research Institute Brain and Body
560 Donation Program of Sun City, Arizona for the provision of human biological materials. The
561 Brain and Body Donation Program is supported by the National Institute of Neurological
562 Disorders and Stroke (U24 NS072026 National Brain and Tissue Resource for Parkinson's
563 Disease and Related Disorders), the National Institute on Aging (P30 AG19610 Arizona
564 Alzheimer's Disease Core Center), the Arizona Department of Health Services (contract 211002,
565 Arizona Alzheimer's Research Center), the Arizona Biomedical Research Commission (contracts
566 4001, 0011, 05-901 and 1001 to the Arizona Parkinson's Disease Consortium) and the Michael J.
567 Fox Foundation for Parkinson's Research.
568
569 **COMPETING FINANCIAL INTERESTS**
570 The authors declare that they have no competing financial interests.
571

REFERENCES

1. Shah, V. *et al.* Enhanced data-independent analysis of lipids using ion mobility-TOFMS(E) to unravel quantitative and qualitative information in human plasma. *Rapid communications in mass spectrometry : RCM* **27**, 2195-2200 (2013).
2. Hart, P.J., Francese, S., Claude, E., Woodroofe, M.N. & Clench, M.R. MALDI-MS imaging of lipids in ex vivo human skin. *Analytical and bioanalytical chemistry* **401**, 115-125 (2011).
3. Damen, C.W., Isaac, G., Langridge, J., Hankemeier, T. & Vreeken, R.J. Enhanced lipid isomer separation in human plasma using reversed-phase UPLC with ion-mobility/high-resolution MS detection. *Journal of lipid research* **55**, 1772-1783 (2014).
4. Kim, H.I. *et al.* Structural characterization of unsaturated phosphatidylcholines using traveling wave ion mobility spectrometry. *Analytical chemistry* **81**, 8289-8297 (2009).
5. Castro-Perez, J. *et al.* Localization of fatty acyl and double bond positions in phosphatidylcholines using a dual stage CID fragmentation coupled with ion mobility mass spectrometry. *Journal of the American Society for Mass Spectrometry* **22**, 1552-1567 (2011).
6. Kaur-Atwal, G. *et al.* Determination of testosterone and epitestosterone glucuronides in urine by ultra performance liquid chromatography-ion mobility-mass spectrometry. *The Analyst* **136**, 3911-3916 (2011).
7. Ahonen, L. *et al.* Separation of steroid isomers by ion mobility mass spectrometry. *Journal of chromatography. A* **1310**, 133-137 (2013).
8. Dong, L. *et al.* Collision Cross-Section Determination and Tandem Mass Spectrometric Analysis of Isomeric Carotenoids Using Electrospray Ion Mobility Time-of-Flight Mass Spectrometry. *Analytical chemistry* (2010).
9. Domalain, V. *et al.* Use of transition metals to improve the diastereomers differentiation by ion mobility and mass spectrometry. *Journal of mass spectrometry : JMS* **49**, 423-427 (2014).
10. Malkar, A.D., N.A.; Martin, H.J.; Patel, P.; Turner, M.A.; Watson, P.; Maughan, R.J.; Reid, H.J.; Sharp, B.L.; Thomas, C.L.P.; Reynolds, J.C.; Creaser, C.S. Metabolic profiling of human saliva

before and after induced physiological stress by ultra-high performance liquid chromatography–ion mobility–mass spectrometry. *Metabolomics* **9**, 1192-1201 (2013).

11. Dwivedi, P., Schultz, A.J. & Hill, H.H. Metabolic Profiling of Human Blood by High Resolution Ion Mobility Mass Spectrometry (IM-MS). *International journal of mass spectrometry* **298**, 78-90 (2010).

12. Dwivedi, P. *et al.* Metabolic profiling of Escherichia coli by ion mobility-mass spectrometry with MALDI ion source. *Journal of mass spectrometry : JMS* **45**, 1383-1393 (2010).

13. Kaplan, K. *et al.* Monitoring dynamic changes in lymph metabolome of fasting and fed rats by electrospray ionization-ion mobility mass spectrometry (ESI-IMMS). *Analytical chemistry* **81**, 7944-7953 (2009).

14. Harry, E.L., Weston, D.J., Bristow, A.W., Wilson, I.D. & Creaser, C.S. An approach to enhancing coverage of the urinary metabonome using liquid chromatography-ion mobility-mass spectrometry. *Journal of chromatography. B, Analytical technologies in the biomedical and life sciences* **871**, 357-361 (2008).

15. Lapthorn, C., Pullen, F. & Chowdhry, B.Z. Ion mobility spectrometry-mass spectrometry (IMS-MS) of small molecules: separating and assigning structures to ions. *Mass spectrometry reviews* **32**, 43-71 (2013).

16. May, J.C. & McLean, J.A. Ion mobility-mass spectrometry: time-dispersive instrumentation. *Analytical chemistry* **87**, 1422-1436 (2015).

17. Kanu, A.B., Dwivedi, P., Tam, M., Matz, L. & Hill, H.H., Jr. Ion mobility-mass spectrometry. *Journal of mass spectrometry : JMS* **43**, 1-22 (2008).

18. Lanucara, F., Holman, S.W., Gray, C.J. & Eyers, C.E. The power of ion mobility-mass spectrometry for structural characterization and the study of conformational dynamics. *Nature chemistry* **6**, 281-294 (2014).

19. Chong, W.P. *et al.* Metabolomics profiling of extracellular metabolites in recombinant Chinese Hamster Ovary fed-batch culture. *Rapid communications in mass spectrometry : RCM* **23**, 3763-3771 (2009).
20. Paglia, G. *et al.* Ion-Mobility-Derived Collision Cross Section as an Additional Measure for Lipid Fingerprinting and Identification. *Analytical chemistry* **87**, 1137-1144 (2015).
21. Pacini, T. *et al.* Multidimensional analytical approach based on UHPLC-UV-ion mobility-MS for the screening of natural pigments. *Analytical chemistry* **87**, 2593-2599 (2015).
22. Paglia, G. *et al.* Ion mobility derived collision cross sections to support metabolomics applications. *Analytical chemistry* **86**, 3985-3993 (2014).
23. Ibrahim, Y.M. *et al.* Development of a New Ion Mobility (Quadrupole) Time-of-Flight Mass Spectrometer. *International journal of mass spectrometry* **377**, 655-662 (2015).
24. Giles, K. Travelling wave ion mobility. *International Journal For Ion Mobility Spectrometry* (2013).
25. Shvartsburg, A.A. & Smith, R.D. Fundamentals of traveling wave ion mobility spectrometry. *Analytical chemistry* **80**, 9689-9699 (2008).
26. Shvartsburg, A.A. *Differential Mobility Spectrometry: Nonlinear Ion Transport and Fundamentals of FAIMS*. (CRC Press, 2008).
27. Michelmann, K., Silveira, J.A., Ridgeway, M.E. & Park, M.A. Fundamentals of trapped ion mobility spectrometry. *Journal of the American Society for Mass Spectrometry* **26**, 14-24 (2015).
28. Hernandez, D.R. *et al.* Ion dynamics in a trapped ion mobility spectrometer. *The Analyst* **139**, 1913-1921 (2014).
29. Fernandez-Lima, F., Kaplan, D.A., Suetering, J. & Park, M.A. Gas-phase separation using a trapped ion mobility spectrometer. *International journal for ion mobility spectrometry : official publication of the International Society for Ion Mobility Spectrometry* **14** (2011).
30. Baker, P.R., Armando, A.M., Campbell, J.L., Quehenberger, O. & Dennis, E.A. Three-dimensional enhanced lipidomics analysis combining UPLC, differential ion mobility

spectrometry, and mass spectrometric separation strategies. *Journal of lipid research* **55**, 2432-2442 (2014).

31. Lintonen, T.P. *et al.* Differential mobility spectrometry-driven shotgun lipidomics. *Analytical chemistry* **86**, 9662-9669 (2014).

32. Ruotolo, B.T., Benesch, J.L., Sandercock, A.M., Hyung, S.J. & Robinson, C.V. Ion mobility-mass spectrometry analysis of large protein complexes. *Nature protocols* **3**, 1139-1152 (2008).

33. Michaelevski, I., Kirshenbaum, N. & Sharon, M. T-wave ion mobility-mass spectrometry: basic experimental procedures for protein complex analysis. *Journal of visualized experiments : JoVE* (2010).

34. May, J.C. *et al.* Conformational ordering of biomolecules in the gas phase: nitrogen collision cross sections measured on a prototype high resolution drift tube ion mobility-mass spectrometer. *Analytical chemistry* **86**, 2107-2116 (2014).

35. Paglia, G., Kliman, M., Claude, E., Geromanos, S. & Astarita, G. Applications of ion-mobility mass spectrometry for lipid analysis. *Analytical and bioanalytical chemistry* **407**, 4995-5007 (2015).

36. Paglia, G. *et al.* Unbiased Metabolomic Investigation of Alzheimer's Disease Brain Points to Dysregulation of Mitochondrial Aspartate Metabolism. *Journal of proteome research* **15**, 608-618 (2016).

37. Fahy, E. *et al.* Update of the LIPID MAPS comprehensive classification system for lipids. *Journal of lipid research* **50 Suppl**, S9-14 (2009).

38. Quehenberger, O. *et al.* Lipidomics reveals a remarkable diversity of lipids in human plasma. *Journal of lipid research* **51**, 3299-3305 (2010).

39. Quehenberger, O. & Dennis, E.A. The human plasma lipidome. *The New England journal of medicine* **365**, 1812-1823 (2011).

40. Wenk, M.R. The emerging field of lipidomics. *Nature reviews. Drug discovery* **4**, 594-610 (2005).

41. Witting, M., Maier, T.V., Garvis, S. & Schmitt-Kopplin, P. Optimizing a ultrahigh pressure liquid chromatography-time of flight-mass spectrometry approach using a novel sub-2mum core-shell particle for in depth lipidomic profiling of Caenorhabditis elegans. *Journal of chromatography. A* **1359**, 91-99 (2014).

42. Brown, H.A.M., R.C. Working towards an exegesis for lipids in biology. *Nature chemical biology* **5**, 602-606 (2009).

43. Shevchenko, A. & Simons, K. Lipidomics: coming to grips with lipid diversity. *Nature reviews. Molecular cell biology* **11**, 593-598 (2010).

44. Fenn, L.S., Kliman, M., Mahsut, A., Zhao, S.R. & McLean, J.A. Characterizing ion mobility-mass spectrometry conformation space for the analysis of complex biological samples. *Analytical and bioanalytical chemistry* **394**, 235-244 (2009).

45. Kliman, M., May, J.C. & McLean, J.A. Lipid analysis and lipidomics by structurally selective ion mobility-mass spectrometry. *Biochimica et biophysica acta* **1811**, 935-945 (2011).

46. Woods, A.S. *et al.* Lipid/peptide/nucleotide separation with MALDI-ion mobility-TOF MS. *Analytical chemistry* **76**, 2187-2195 (2004).

47. Jackson, S.N. *et al.* A study of phospholipids by ion mobility TOFMS. *Journal of the American Society for Mass Spectrometry* **19**, 1655-1662 (2008).

48. Shvartsburg, A.A., Isaac, G., Leveque, N., Smith, R.D. & Metz, T.O. Separation and classification of lipids using differential ion mobility spectrometry. *Journal of the American Society for Mass Spectrometry* **22**, 1146-1155 (2011).

49. Leng, J. *et al.* Direct infusion electrospray ionization-ion mobility-mass spectrometry for comparative profiling of fatty acids based on stable isotope labeling. *Analytica chimica acta* **887**, 148-154 (2015).

50. Skraskova, K. *et al.* Enhanced capabilities for imaging gangliosides in murine brain with matrix-assisted laser desorption/ionization and desorption electrospray ionization mass spectrometry coupled to ion mobility separation. *Methods* (2016).

51. Silveira, J.A., Ridgeway, M.E. & Park, M.A. High resolution trapped ion mobility spectrometery of peptides. *Analytical chemistry* **86**, 5624-5627 (2014).

52. Mason, E.A.M., E.W. *Transport Properties of Ions in Gases*. (John Wiley, 1998).

53. Zhang, F., Guo, S., Zhang, M., Zhang, Z. & Guo, Y. Characterizing ion mobility and collision cross section of fatty acids using electrospray ion mobility mass spectrometry. *Journal of mass spectrometry : JMS* **50**, 906-913 (2015).

54. Williams, J.P. *et al.* Isomer separation and gas-phase configurations of organoruthenium anticancer complexes: ion mobility mass spectrometry and modeling. *Journal of the American Society for Mass Spectrometry* **20**, 1119-1122 (2009).

55. Bush, M.F., Campuzano, I.D. & Robinson, C.V. Ion mobility mass spectrometry of peptide ions: effects of drift gas and calibration strategies. *Analytical chemistry* **84**, 7124-7130 (2012).

56. Campuzano, I. *et al.* Structural characterization of drug-like compounds by ion mobility mass spectrometry: comparison of theoretical and experimentally derived nitrogen collision cross sections. *Analytical chemistry* **84**, 1026-1033 (2012).

57. Gonzales, G.B. *et al.* Ultra(high)-pressure liquid chromatography-electrospray ionization-time-of-flight-ion mobility-high definition mass spectrometry for the rapid identification and structural characterization of flavonoid glycosides from cauliflower waste. *Journal of chromatography. A* **1323**, 39-48 (2014).

58. Dear, G.J. *et al.* Sites of metabolic substitution: investigating metabolite structures utilising ion mobility and molecular modelling. *Rapid communications in mass spectrometry : RCM* **24**, 3157-3162 (2010).

59. Giles, K. *et al.* Applications of a travelling wave-based radio-frequency-only stacked ring ion guide. *Rapid communications in mass spectrometry : RCM* **18**, 2401-2414 (2004).

60. Wishart, D.S. *et al.* HMDB 3.0--The Human Metabolome Database in 2013. *Nucleic acids research* **41**, D801-807 (2013).

61. Kind, T. *et al.* LipidBlast in silico tandem mass spectrometry database for lipid identification. *Nature methods* **10**, 755-758 (2013).

62. Smith, C.A. *et al.* METLIN: a metabolite mass spectral database. *Therapeutic drug monitoring* **27**, 747-751 (2005).

63. Hines, K.M., May, J.C., McLean, J.A. & Xu, L. Evaluation of Collision Cross Section Calibrants for Structural Analysis of Lipids by Traveling Wave Ion Mobility-Mass Spectrometry. *Analytical chemistry* **88**, 7329-7336 (2016).

64. Menikarachchi, L.C. *et al.* MolFind: a software package enabling HPLC/MS-based identification of unknown chemical structures. *Analytical chemistry* **84**, 9388-9394 (2012).

FIGURE LEGENDS

Table 1. Comparison of the four main types of IMS-MS technologies commercially available.

Table 2. List of commercially available natural lipids and lipid extracts

Table 3. Collision cross-sections (CCS) for singly charged, protonated and deprotonated oligomers of poly-DL-alanine, in nitrogen.

Table 4. Representative TWIMS-MS settings for polar metabolites analysis.

Table 5. Representative TWIMS Settings for lipid analysis.

Table 6. Troubleshooting.

Figure 1. Ion-mobility spectrometry (IMS) mass spectrometry (MS) can be used with traditional lipidomic approaches, such as chromatography, (e.g. liquid chromatography). Independently from the inlet source and the ionization mode, lipid and metabolite ions are separated before MS detection by their drift time, which is determined by their charge, size, and shape. Drift-time information can be converted to collision cross section (CCS), a measure of the shape of molecules. CCS provides an additional coordinate for identifying and increasing the signal-to-noise ratio. Compact circle represent sterols and open circle represent phospholipids.

Figure 2. Lipids and metabolites classes can be separated into distinct trend lines by using mass mobility correlation curves. a) mass mobility correlation curves for lipid species. b) mass mobility correlation curves for small polar metabolites. Panel a, reproduced, with permission[20], American Chemical Society. Panel b reproduced, with permission[22], American Chemical Society.

Figure 3. Protocol workflow.

Figure 4. Expected Results. a) Typical UPLC-HDMS chromatogram and 2D plot (drift time vs retention time) obtained from injection of brain (porcine) lipid extract in positive mode. b) Lipid identification is achieved by searching features in database using *m/z* and CCS values. Raw file available at ftp://PASS00928:TWIMMS@ftp.peptideatlas.org/.

Figure 5. Lipid confirmation by using $HDMS^E$ data. a) Data-independent acquisition data, without ion mobility, provides complex mass spectra resulting from co-elution of different PE species at the same retention time. b) by coupling ion mobility with data independent acquisition ($HDMS^E$), coeluting species are separated by ion mobility and mass spectra obtained at high energy provide detailed information about fragment ions, allowing reconfirmation of PE (18:0/22:6). Low energy spectra (in blue) provide accurate mass information of the precursor ions (in red), without any fragmentation information. High energy spectra (in green) provide accurate mass information of the fragments. The high energy is applied post ion mobility separation.

768

Table 1. Comparison of the four main types of IM-MS technologies commercially available.

	DTIMS	TWIMS	FAIMS and DMS	TIMS
Examples of commercially available devices	6560 Ion Mobility Q-TOF LC/MS (Agilent)[23]	SYNAPT High Definition MS[24, 25]	SelexION[26]	timsTOF (Bruker)[27, 29]
Year of release	2014	2006	2012	2016
MS system compatibility	Time-of-flight	Time-of-flight	Triple Quadrupole, linear ion trap and time-of-flight	Time-of-flight
Resolving Power	□ 60-70	□ 40	□20*	□200
Electric field applied	Uniform electrostatic field	Stepped-waveforms	Scanning of radio	Opposite electric field
CCS measurement	Available	Available after calibration with compounds of known CCS	Not available**	Available after calibration with compounds of known CCS
IM separation of fragment ions	Not available	Available in particular instrument configurations such as SYNAPT	Not available	Not available

* Small volumes of chemical modifier in the carrier gas has been demonstrated to significantly increase the resolution and selectivity of mobility separation[30, 31, 40]

**FAIMS devices are not able to preserve the structure of the ions[26]

769

770

Table 2. List of commercially available natural lipids and lipid extracts.

Natural lipids	**Abbreviation**	**Avanti Catalog**
L-phosphatidylcholine (brain, porcine)	PC	840053
L-phosphatidylethanolamine (brain, porcine)	PE	840022
L-lysophosphatidylcholine (egg, chicken)	LPC	830071
L-lysophosphatidylethanolamine plasmalogen (brain, porcine)	LPE	850095
L- phosphatidylinositol (liver, bovine)	PI	840042
L-phosphatidylserine (brain, porcine)	PS	840032
L-phosphatidylglycerol (egg, chicken)	PG	841138
Ceramide (brain, porcine)	Cer	860052
Sphingomyelin (brain, porcine)	SM	860062
Cerebrosides (brain, porcine)	HexCer	131303
Sulfatides (brain, porcine)	ST	131305
Lipid Extracts	Avanti catalogue number	
Brain, porcine	131101	
Heart, bovine	171201	
Liver, bovine	181104	
E. Coli	100500	
Yeast (S. cerevisiae)	190000	

Table 3. Collision cross-sections (CCS) for singly charged protonated and deprotonated oligomers of poly-DL-alanine in nitrogen.

Sequence	MW	Positive		Negative	
		$[M+H]^+$	CCS (Å^2)	$[M-H]^-$	CCS (Å^2)
A_3	231.122	232.13	151	230.114	150
A_4	302.159	303.167	166	301.151	165
A_5	373.196	374.204	181	372.188	179
A_6	444.233	445.241	195	443.225	195
A_7	515.27	516.278	211	514.262	209
A_8	586.307	587.315	228	585.3	223
A_9	657.345	658.352	243	656.337	238
A_{10}	728.382	729.39	256	727.374	253
A_{11}	799.419	800.427	271	798.411	267
A_{12}	870.456	871.464	282	869.448	279
A_{13}	941.493	942.501	294	940.485	294
A_{14}	1012.53	1013.538	306	1011.522	308

Table 4. Representative TWIM-MS settings for small polar metabolites analysis

Polarity	Capillary Volatage	Cone Voltage	Source Temperature	Desolvation Temperature	Desolvation Gas Flow	Cone Gas Flow	EDC Delay Coefficient	Optic Mode	MS Scan Rate	Lock Mass Solution	Lock Mass Flow Rate
ES+	2.2	40 V	110 (°C)	450 (°C)	450 (L/hr)	20	1.58 V	Resolution	0.2 Scan/s	Leu Enk (2 µg/mL)	15 µL/min
ES-	2.2	30 V	110 (°C)	500 (°C)	600 (L/hr)	20	1.58 V	Resolution	0.2 Scan/s	Leu Enk (2 µg/mL)	15 µL/min

Polarity	Triwave DC										
	Trap DC				IMS DC					Transfer DC	
	Entrance	Bias	Trap DC	Exit	Entrance	Helium Cell DC	Helium Exit	Bias	Exit	Entrance	Exit
ES+	3	60	0	3	25	35	-5	3	0	3	3
ES-	3	60	0	3	25	35	-5	3	0	3	3

Polarity	Gas Controls		Triwave					
	IMS gas (Nitrogen)	Helium Cell	Trap		IMS		Tranfer	
			Wave Velocity	Wave Height	Wave Velocity	Wave Height	Wave Velocity	Wave Height
ES+	90 (mL/min)	180 (mL/min)	311 (m/s)	6 (V)	650 (m/s)	40 (V)	220 (m/s)	4 (V)
ES-	90 (mL/min)	180 (mL/min)	311 (m/s)	6 (V)	650 (m/s)	40 (V)	220 (m/s)	4 (V)

Table 5. Representative TWIM-MS settings for lipids analysis

Polarity	Capillary Volatage	Cone Voltage	Source Temperature	Desolvation Temperature	Desolvation Gas Flow	Cone Gas Flow	EDC Delay Coefficient	Optic Mode	MS Scan Rate	Lock Mass Solution	Lock Mass Flow Rate
ES+	2.5	40 V	120 (°C)	500 (°C)	1000 (L/hr)	50	1.58 V	Resolution	0.2 Scan/s	Leu Enk (2 µg/mL)	15 µL/min
ES-	2.5	30 V	120 (°C)	500 (°C)	1000 (L/hr)	50	1.58 V	Resolution	0.2 Scan/s	Leu Enk (2 µg/mL)	15 µL/min

Polarity	Triwave DC										
	Trap DC				IMS DC					Transfer DC	
	Entrance	Bias	Trap DC	Exit	Entrance	Helium Cell DC	Helium Exit	Bias	Exit	Entrance	Exit
ES+	3	60	0	3	25	35	-5	3	0	3	3
ES-	3	60	0	3	25	35	-5	3	0	3	3

Polarity	Gas Controls		Triwave					
	IMS gas (Nitrogen)	Helium Cell	Trap		IMS		Tranfer	
			Wave Velocity	Wave Height	Wave Velocity	Wave Height	Wave Velocity	Wave Height
ES+	90 (mL/min)	180 (mL/min)	311 (m/s)	4 (V)	900 (m/s)	40 (V)	191 (m/s)	4 (V)
ES-	90 (mL/min)	180 (mL/min)	311 (m/s)	4 (V)	900 (m/s)	40 (V)	191 (m/s)	4 (V)

Table 6. Troubleshooting

Step	Problem	Possible reason	Solution
1Aiv, 1Biv	Separation of isomers and isobaric compounds is not achieved	TWIMS resolution is insufficient	Change the pressure of the TWIMS gas. Derivatization methods can be used to maximize the separation of isobaric and isomeric lipid species by TWIM-MS. The derivatization increases the CCS of the isomers, affecting the interactions of the lipid ion with the drift gas and thus improving their separation in the ion-mobility cell. Alternative ion-mobility gases can maximize the effect of separating isobaric and isomeric lipid species by TWIM-MS. Gases of different polarizabilities can enhance the resolution of isomers. CCS can be derived only by using nitrogen and helium, as TWIMS gases.
1Aiv, 1Biv	Ion mobility signal in the Tune window is distorted or diagonal strips appear in 2D (drift time vs retention time) plots	TWIMS settings are not optimized. Transfer T-wave/ToF pusher aliasing due to partial synchronization between the Transfer T-wave and the ToF pusher.	Infuse leukine enkephalin without changing the TWIM-MS settings of the analysis. If the ion mobility signal is distorted and you can see aliasing phenomenon, change the transfer T-wave velocity by ±1 ms until aliasing is minimized and the signal for leukine-enkephalin is stable and undistorted.
1Aiv, 1Biv	Same ion peaks are detected at the beginning and at the end of the driftogram	TWIMS settings are not optimized. As result, a new ion packet is released from the Trap region before the previous packet has been delivered to the pusher region.	Increase T-wave height, and decreasing T-wave velocity in the TWIMS cell.
2	poly-DL-alanine does not dissolve in acetonitrile-water solution	poly-DL-alanine product not correct	Ensure that you are using poly-DL-alanine (Sigma cat. No. p9003). Other poly-alanine products might not fully dissolve in acetonitrile/water (50:50).
5, 6	CCS values are not correct	CCS calibration not correct	Check that poly-DL-Alanine was acquired using the exact same TWIMS settings used for standard acquisition.
		CCS calibration not correct	Perform CCS calibration (Step 2, 3 and 4) using CCS Major mix calibration solution instead of poly-DL-alanine. This calibration mix has reference masses for molecular weights lower than 200 Da and

			perform better for deriving CCS for small metabolites.
		CCS calibration not correct	One of the limitations of such an approach is that peptides have unique physical properties and gas-phase conformations, which makes the calibration with poly-DL-alanine may not be ideal to calculate the accurate CCS values for all metabolites and lipids classes. Alternative calibrants have been proposed for lipids, which better reflect their chemical structure[63].
		EDC delay value not correct	Check that in your acquisition setting the EDC delay value is the same used in the same used for calculating the corrected drift time in step 10.
		Presence of unresolved isomers	The TWIMS resolution of a SYNAPT HDMS instrument is tuned to ~40 (FWHM). The TWIMS peak or arrival time distribution (ATD) may represent a combination of structurally similar isomers that remain unresolved at that resolution.
		Differences due to the use of different ionization sources	The CCS values reported are determined at the apex of the TWIMS peak or ATD. The use of different ionization sources or different mobility calibrants could lead to slight variations in the reported CCS values.
19	No match with CCS database	Compound not present in the database	Use MobCal for calculating theoretical CCS for tentatively identified metabolites not present in the database[22, 64].
30	CCS values during TAP fragmentation experiments are not correct	CCS calibration not correct	If you have changed TWIMS setting to better separate fragment ions during TAP experiment you need to perform a new CCS calibration. Perform step 9 using the new TWIM-MS settings.

829

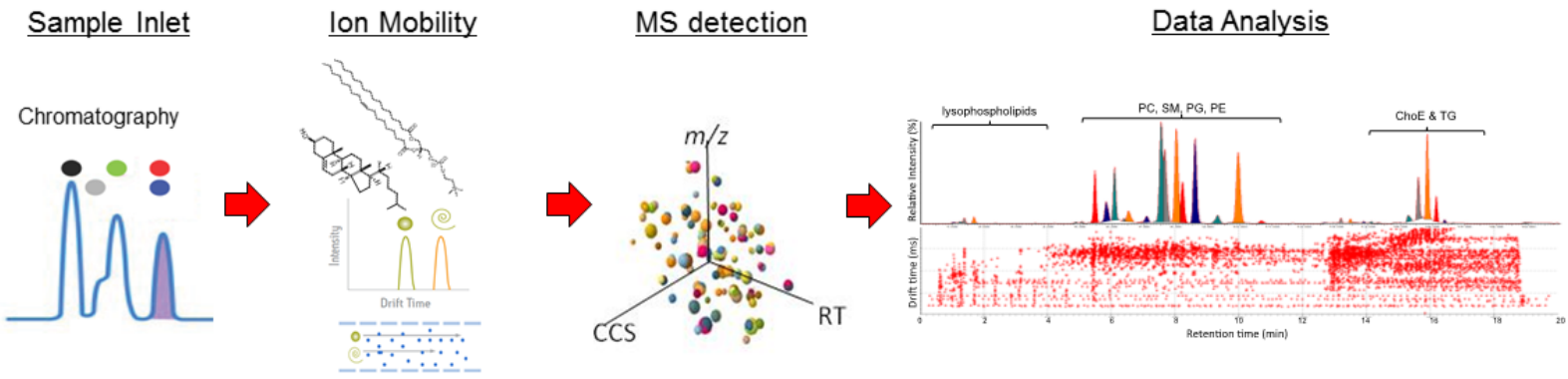
Sample Inlet
Chromatography
Ion Mobility
Intensity
Drift Time
MS detection
m/z
CCS
RT
Data Analysis
lysophospholipids
PC, SM, PG, PE
ChoE & TG
Relative Intensity (%)
Drift time (ms)
Retention time (min)

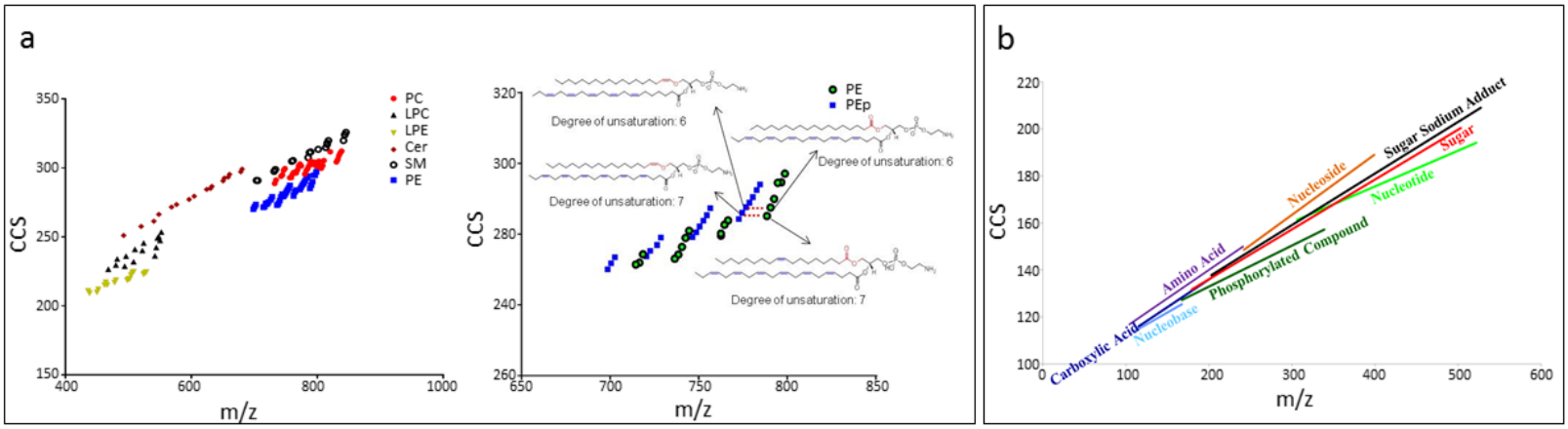
a
CCS
m/z
PC
LPC
LPE
Cer
SM
PE
PEp
Degree of unsaturation: 6
Degree of unsaturation: 7
Degree of unsaturation: 6
Degree of unsaturation: 7
b
CCS
m/z
Carboxylic Acid
Amino Acid
Nucleobase
Nucleoside
Phosphorylated Compound
Nucleotide
Sugar
Sugar Sodium Adduct

IM-MS Tuning and CCS calibration

- Optimize IM-MS settings for metabolomics and/or lipidomics
- Generate CCS calibration curve using optimized IM-MS settings

Sample Treatment

- Extract lipids and metabolites from tissue using liquid/liquid extraction
- Separate Upper Phase (Polar Metabolites) from Lower Phase (Lipids)

UHPLC-HDMS^E

- Prepare the UHPLC-IM-MS system.
- Use HILIC for Polar Metabolites and RP Chromatography for lipids
- Run yours Samples and QCs

Data Analysis

- Extract features, characterized by three coordinates, *m/z*, RT and CCS
- Match Features with Database for lipids/metabolites identification

Confirm Metabolites

- Use function acquired at High Energy during your HDMS^E experiment to confirm metabolites using characteristic fragment ions
- Perform time alligned parallel fragmentation experiments to identify unknown compounds

a

UPLC-HDMS^E analysis

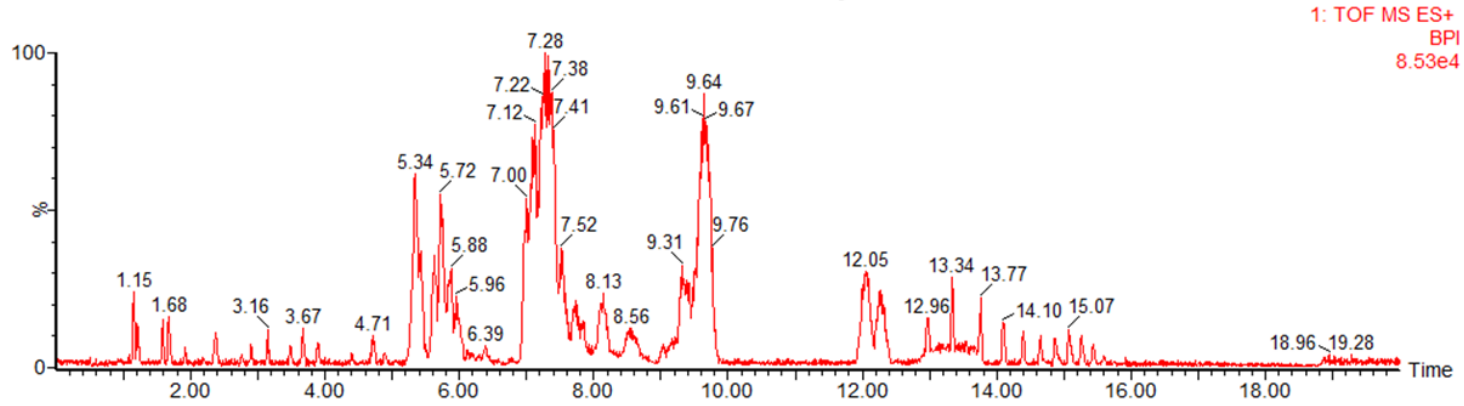

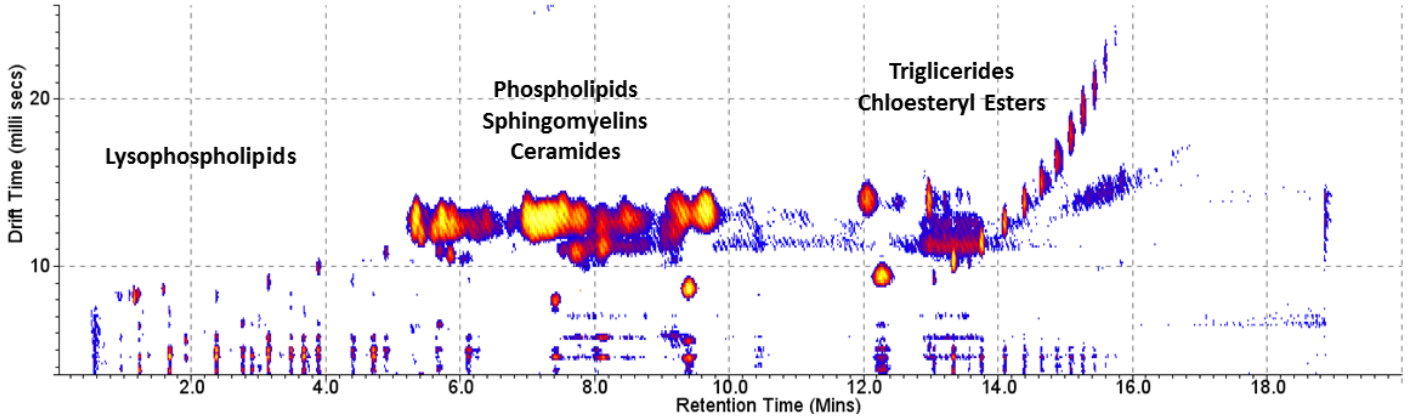

b

Lipid Identification

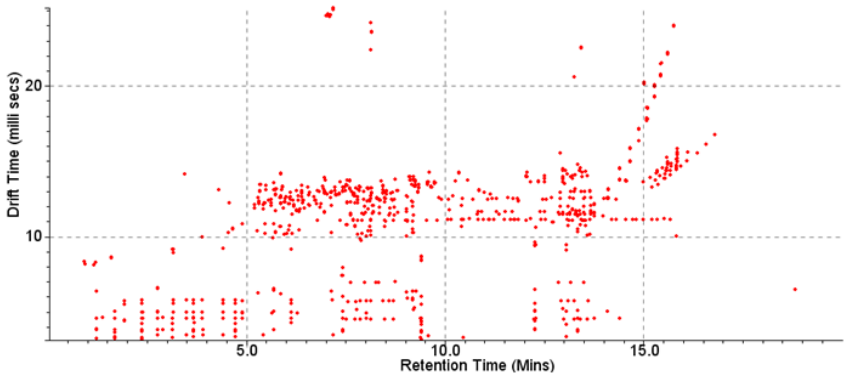

m/z	RT (min)	CCS (Å^2)	Δ ppm	Δ CCS	Database Match
522.3558	1.21	237	0.8	-1.3	LC 18:1
731.6072	7	294	1.4	-1	SM d18:1/18:0
758.5700	6.31	295	0.8	0.7	PC 34:2

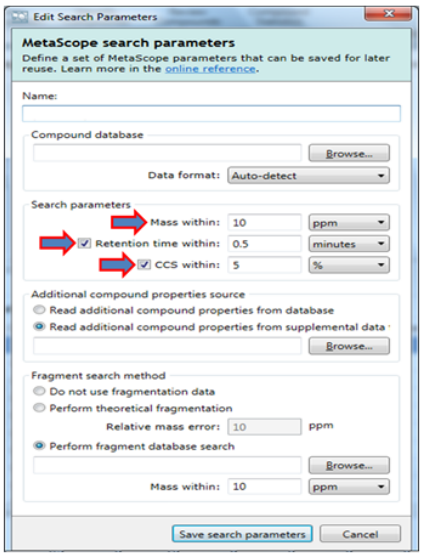

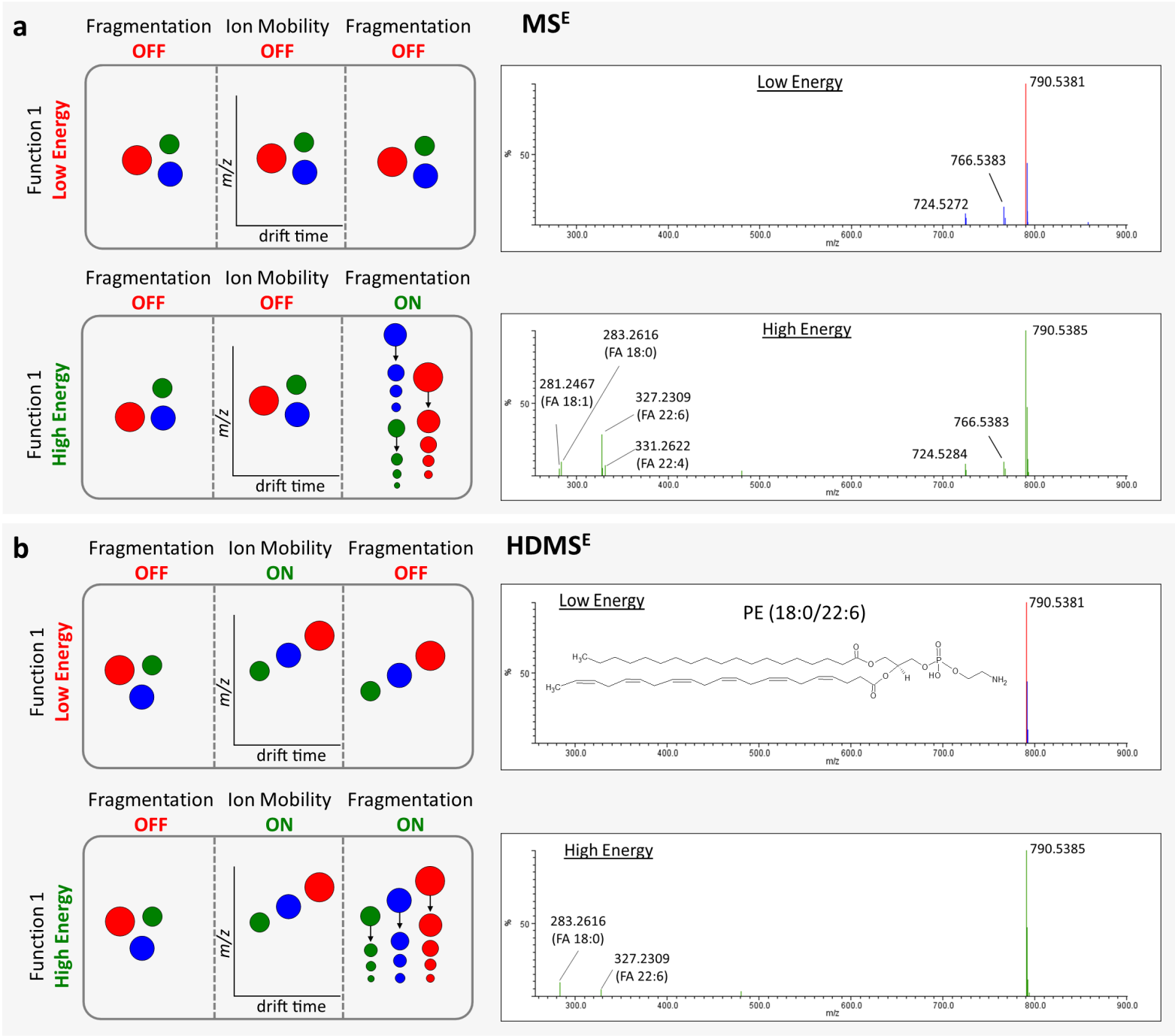
a
Fragmentation
Ion Mobility
Fragmentation
OFF
OFF
OFF
Function 1
Low Energy
m/z
drift time
MS^E
Low Energy
790.5381
766.5383
724.5272
Fragmentation
Ion Mobility
Fragmentation
OFF
OFF
ON
Function 1
High Energy
m/z
drift time
High Energy
283.2616
(FA 18:0)
281.2467
(FA 18:1)
327.2309
(FA 22:6)
331.2622
(FA 22:4)
790.5385
766.5383
724.5284
b
Fragmentation
Ion Mobility
Fragmentation
OFF
ON
OFF
Function 1
Low Energy
m/z
drift time
HDMS^E
Low Energy
PE (18:0/22:6)
790.5381
Fragmentation
Ion Mobility
Fragmentation
OFF
ON
ON
Function 1
High Energy
m/z
drift time
High Energy
283.2616
(FA 18:0)
327.2309
(FA 22:6)
790.5385
m/z